

Survey of catalytic performance of TiO₂ via coupling with ZSM-5 Zeolite under UV light for activation of peroxymonosulfate Applied towards Orange II (OII) degradation

Parisa Nasrollahi¹, Seyyed Abbas Mirzaee^{2,3}, Zeinab Gholami², Mohsen Mansouri¹, Zahra Noorimotlagh²

¹Department of Chemical Engineering, Ilam University, Ilam, Iran

²Health and Environment Research Center, Ilam University of Medical Sciences, Ilam, Iran

³Department of Environmental Health Engineering, School of Health, Ilam University of Medical Sciences, Ilam, Iran

Abstract

Background: The widespread presence of organic dyes in the various industries' effluent such as paper, textile, and clothing has led to significant environmental pollution. Titanium oxide (TiO₂) nanoparticles immobilized on zeolite (ZSM-5) were investigated under UV light for activation of peroxymonosulfate (PMS) for photocatalytic degradation of Orange II (OII) dye in aqueous solutions.

Methods: In this study, the photocatalyst used was prepared by immobilizing different amounts of TiO₂ nanoparticles on ZSM-5. Characterization analyses including X-ray diffractometer (XRD), Fourier transform infrared (FTIR), BET, scanning electron microscope (SEM), and energy dispersive X-ray spectroscopy (EDS) were performed on the synthesized samples. Then, the effect of various parameters, such as TiO₂ nanoparticles loading onto the ZSM-5, pH, contact time, dye concentration, and TiO₂/ZSM-5 dosage, is investigated for the removal of OII as a model molecule under the UV irradiation with 15 W power.

Results: The highest removal percentage of OII dye (97.44%) was obtained in the optimal operating conditions of pH=3, the initial dye concentration = 5 ppm, amount of TiO₂/ZSM-5 = 10 mg/L, amount of PMS = 50 mg/L, and reaction time = 120 minutes. The Langmuir-Hinshelwood kinetics model fitted with the experimental data.

Conclusion: The obtained results of this research showed that PMS can be used as a suitable oxidant activated with ZSM-5/TiO₂ nanocomposite in OII degradation in different water environments, by optimizing the effective operating factors.

Keywords: Coloring agents, Titanium dioxide, Peroxymonosulfate, Textiles, ZSM-5 zeolite

Citation: Nasrollahi P, Mirzaee SA, Gholami Z, Mansouri M, Noorimotlagh Z. Survey of catalytic performance of TiO₂ via coupling with ZSM-5 Zeolite under UV light for activation of peroxymonosulfate Applied towards Orange II (OII) degradation. Environmental Health Engineering and Management Journal 2023; 10(4): 419-428. doi: 10.34172/EHEM.2023.45.

Article History:

Received: 25 January 2023

Accepted: 20 June 2023

ePublished: 27 September 2023

*Correspondence to:

Mohsen Mansouri,
Email: mansouri2010@yahoo.com and
Zahra Noorimotlagh,
Email: Noorimotlagh.Zahra@gmail.com

Introduction

Environmental protection and treatment of industrial effluents are of great importance. The discharge of wastewater from various industries into the environment has irreparable effects on the physical, chemical, and biological characteristics of the environment. Effluent from dye industries is one of the most important factors of water source pollution. Orange II (OII) is one of the acid dyes, which is used in many cosmetic and textile industries (1-3). This substance is toxic and has carcinogenic properties. Therefore, removing OII dye from industrial wastewater is of great importance (1,4-7).

The removal of dye and other contaminants from aquatic environments has become a challenging problem in recent years (8-10). Therefore, various strategies such as ozonation, membrane filtration, biosorption removal

by ion exchange, surface adsorption, advanced oxidation processes (AOPs), catalytic reduction, biological/aerobic treatment, and coagulation have been adopted to remove persistent organic pollutants. Each of these methods, in addition to advantages, has also disadvantages that cause problems in removing dye from the water environment (11-13). For example, although the ozonation process can show a removal efficiency of over 90%, it produces highly toxic by-products (11,14,15).

In recent years, AOPs have been used to remove organic compounds, especially resistant organic compounds (16,17). Among the AOPs, the photocatalytic process using titanium dioxide (TiO₂) has attracted a lot of attention as an efficient and non-toxic method for wastewater treatment (18,19). This catalyst shows high photocatalytic activity; besides, it has good stability and is relatively



cheap. In any case, the use of TiO₂ nanoparticle powder has technical obstacles that prevent its commercialization, and the most important one is the separation and recovery of nanoparticles after purification and at the reactor outlet. To solve this problem, the approach of stabilizing nanoparticles on different materials such as fixing TiO₂ nanoparticles on carriers including quartz, gel, silica, activated carbon, and zeolite can be used (17,19).

Zeolites are suitable bases for heterogeneous catalysts due to their porous structure, different degrees of hydrophobicity, the possibility of controlling acidity, and modifiability through ion exchange (20). Thermal stability, pore structure, acidity, and selectivity have made ZSM-5 Zeolite find many applications in absorption processes, photocatalytic degradation, and petrochemical processes (21).

Peroxymonosulfate (PMS) with an oxidation potential of 2.5-3.1 V is one of the compounds used in the oxidation of organic compounds (16). Cost-effectiveness, non-selective oxidation, high stability of radicals produced from it in different conditions, high solubility, solid form, and thus, ease of handling and storage are the advantages of this substance (22). Several studies have indicated that PMS radicals can degrade organic materials with slow kinetics at room temperature. Therefore, to accelerate the process, UV light and electron transfer by TiO₂ nanoparticles are used to activate the PMS. Sulfate radical production (SO₄^{•-}) with an oxidation potential of 2.6 V is the final product of the activation process (23-25).

In the study of Hao et al., the PMS activation system was made by UV light with multi-walled carbon nanotubes (CNT)-TiO₂ composite catalyst. It was found that under UV light irradiation, induced electrons produced from TiO₂ can be transferred to CNT to activate PMS to improve the catalytic performance of organic pollutants degradation. The higher catalytic performance is attributed to the electrons induced by light, which can increase the activation of PMS by transferring electrons in the UV/PMS/CNT-TiO₂ system (26).

Therefore, this study aimed to remove OII dye using ZSM-5 Zeolite/TiO₂ nanocomposite under UV light for activation of PMS. The effect of various parameters, such as TiO₂ nanoparticles loading onto the ZSM-5, pH, contact time, dye concentration, and TiO₂/ZSM-5 dosage, were investigated for the removal of OII as a model molecule under the UV irradiation with 15 W power.

Materials and Methods

Materials

All materials include OII dye (Acid Orange 7, Orange II, C₁₆H₁₁N₂NaO₄S), zeolite (ZSM-5), PMS (H₂SO₅), nitric acid (HNO₃), sodium hydroxide (NaOH), hydrogen peroxide (H₂O₂), ethylene diamine tetra acetic acid (EDTA), and silver nitrate (AgNO₃) were purchased from Merck, Germany. 2-Propanol and titanium (IV) tetraisopropoxide

(TTIP) were purchased from Sigma-Aldrich.

Synthesis of TiO₂ nanoparticles

TiO₂ nanoparticles were synthesized using the sol-gel technique. First, 30 ml of 2-propanol was mixed with 5 ml of titanium (IV) TTIP by stirring at room temperature for 30 minutes. Then, 5 mL of acetic acid was added to the above clear mixture at room temperature to form a sol, which was then kept at room temperature for 24 hours to ensure complete hydrolysis of the precursors. Then, the obtained sol was spread in distilled water and the sol turned into a gel. Afterward, the cloudy suspension obtained was placed in an oven at 110 °C for 3 hours. The dried product was calcined in an oven at a temperature of 500 °C with a heating rate of 10/min for about 3 hours. Finally, the final product was ground by hand to provide a white powder (19).

Synthesis of ZSM-5/TiO₂ nanocomposite

One gram of ZSM-5 zeolite was measured with different amounts of TiO₂ nanoparticles (50, 100, 150, 200, and 250 mg). Then, the weighted amounts of TiO₂ nanoparticles and ZSM-5 zeolite were poured into a beaker containing 50 ml of distilled water and placed on a magnetic stirrer for 3 h. The obtained mixtures were passed through fiberglass (Whatman 42). The samples were placed in a porcelain crucible and placed in an oven at 250 °C for 70 minutes. The synthesized samples were named TiO₂/ZSM-5 (50), TiO₂/ZSM-5 (100), TiO₂/ZSM-5 (150), TiO₂/ZSM-5 (200), and TiO₂/ZSM-5 (250) (17).

Characterization

To measure the specific surface area (BET), the BELSORP-mini II device (Microtrac Bel Corp., Japan) was used. The estimation of particle size and examination of product morphology was done using the FEI Quanta 200 scanning electron microscope (SEM). Fourier transform infrared spectrometer (FTIR; model Vector 22, Bruker, Germany) was used to check the structure, composition, and assurance of the correct loading of nanoparticles on zeolite. The energy dispersive X-ray spectroscopy (EDS) analysis was performed using the Czech TESCAN MIRA3 device. This section is an extension to SEM. Using an X-ray diffractometer (XRD; model Philips PW 1730) through a Cu-Kα beam (copper cathode), to determine the crystalline structure of the synthesized nanoparticles was investigated.

Photocatalytic activities

One hundred milliliters of OII dye solution with a specific concentration was added to a beaker with a volume of 250 mL. Then, the synthesized samples were added to the desired beaker and stirred for 30 minutes in the dark to reach the equilibrium of surface absorption. In the next step, it was exposed to LED (15 and 30 W) and UVA (15

W) light. The analysis of the final solution was performed by a spectrophotometer with a wavelength of 485 nm. The samples were stirred by a magnet on a magnetic stirrer throughout the degradation period.

Results

Characterization of the catalyst

Figures 1a, 1b and 1c show the XRD patterns of TiO₂ nanoparticles, ZSM-5 zeolite, and ZSM-5/TiO₂ nanocomposite, respectively.

Figures 2a, 2b, and 2c show the spectra related to the FTIR analysis of TiO₂ nanoparticles, ZSM-5 zeolite, and TiO₂/ZSM-5 nanocomposite, respectively.

Table S1 shows the characteristics obtained from ZSM-5 Zeolite (316/20 m²/g) and TiO₂/ZSM-5 (200) (384/54 m²/g) nanocomposite through BET analysis.

Figure S1a and S1b show the diagram of nitrogen adsorption and desorption related to ZSM-5 zeolite and TiO₂/ZSM-5 nanocomposite, respectively. Figures 3a, 3b, 3c, and 3d show images related to the SEM analysis of ZSM-5 samples (a and b) and TiO₂/ZSM-5 (200) nanocomposite. In Figure 3a and 3b, a sample of zeolite can be seen, which has a coffin-shaped structure. Figure 3d shows the presence of TiO₂ in the structure of zeolite ZSM-5. Figure S2 and Figure S3 show the elemental diagram of ZSM-5 zeolite and TiO₂/ZSM-

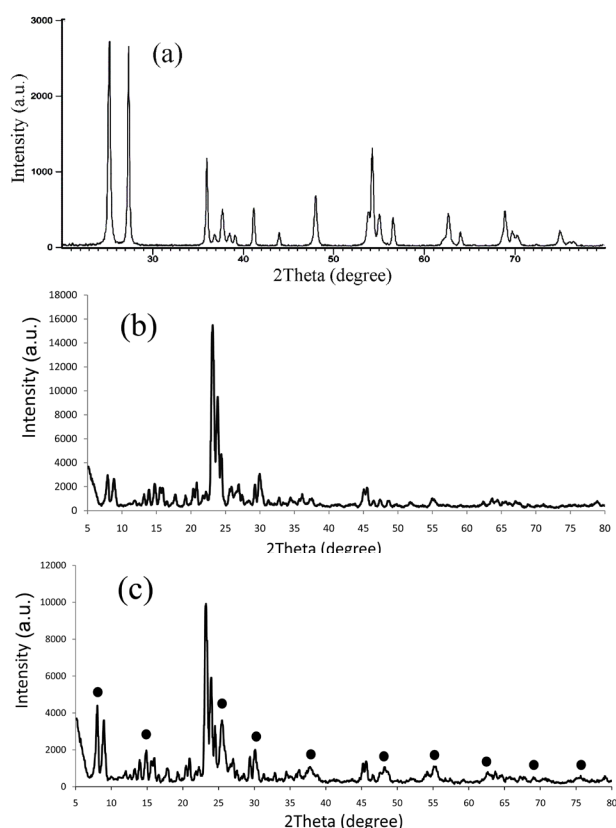


Figure 1. XRD patterns of (a) TiO₂ nanoparticles, (b) ZSM-5 zeolite, and (c) ZSM-5/TiO₂ nanocomposite

5 nanocomposite, respectively. Tables S2-S3 show the information about the mass percentage of zeolite and TiO₂/ZSM-5 nanocomposite, respectively.

Removal of OII

Effect of TiO₂ amount coated on zeolite

Figure 4 shows the effect of TiO₂ on the process efficiency. As shown in this figure, with an increase in the ratio of TiO₂ coated on zeolite, the removal percentage increased, but after reaching a certain value (200 mg of TiO₂ per 1 g of zeolite), this amount decreased. In this experiment, conditions of pH=7, OII concentration=15 ppm, PMS amount=30 mg/L, and ZSM-5/TiO₂ nanocomposite amount=30 mg/L and in the presence of a UV lamp with a power of 15 W, the highest removal percentage was obtained in 120 minutes of reaction.

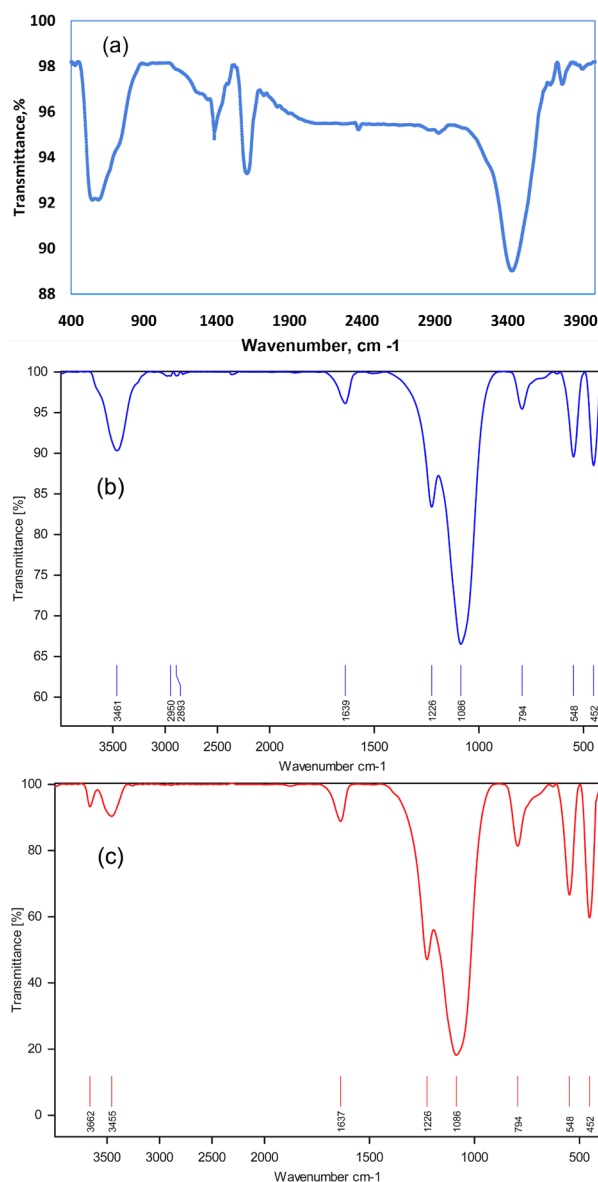


Figure 2. The FTIR spectra of (a) TiO₂ nanoparticles, (b) ZSM-5 zeolite, and (c) ZSM-5/TiO₂ nanocomposite

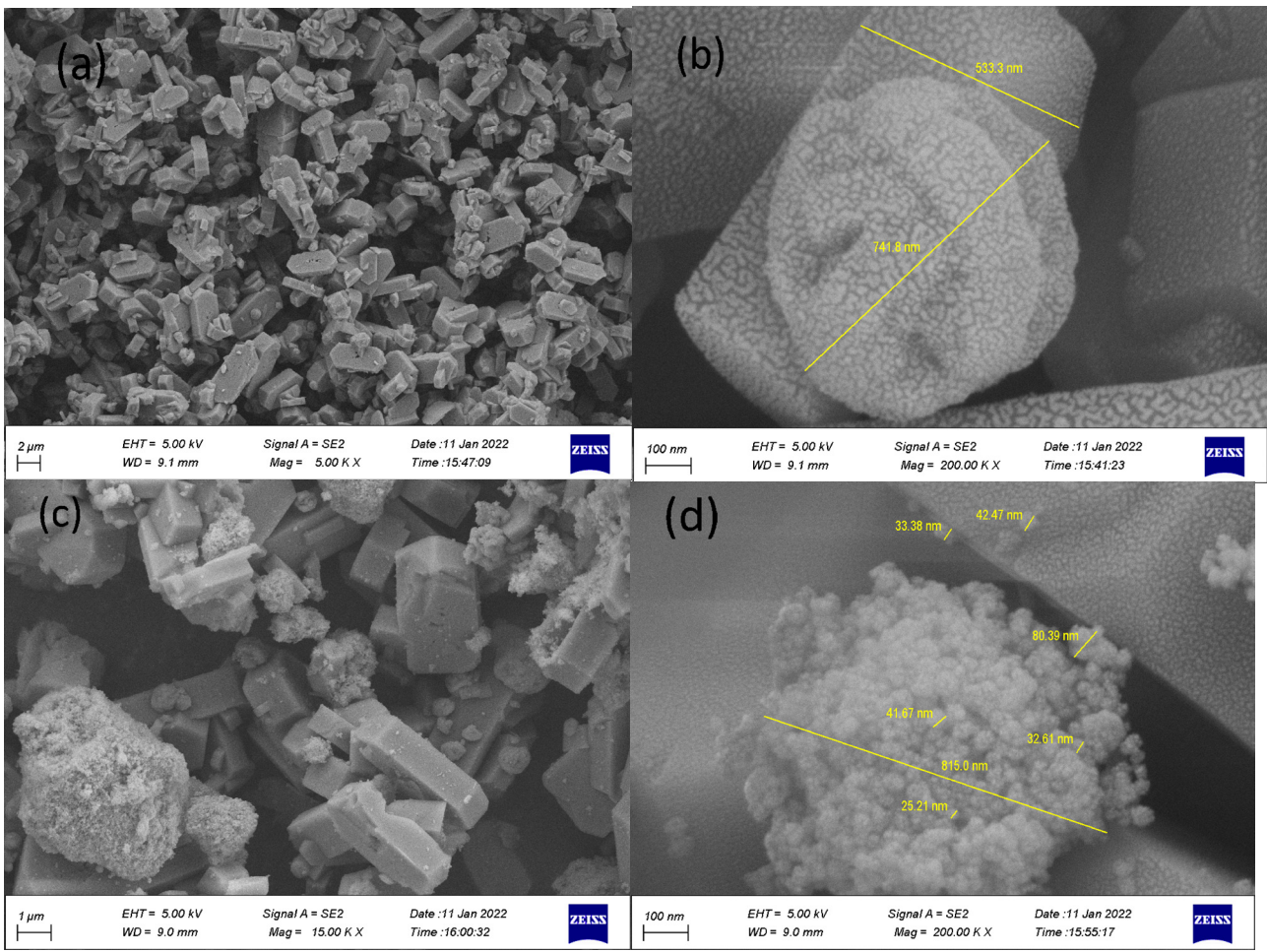


Figure 3. SEM of a & b) ZSM-5 zeolite, c & d) ZSM-5/TiO₂ nanocomposite

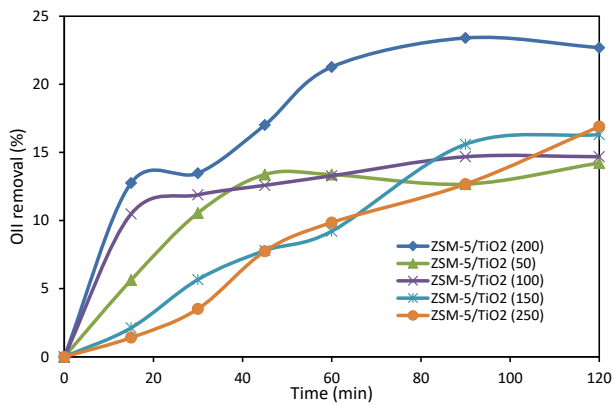


Figure 4. The effect of TiO₂ on process efficiency (the experimental conditions of pH=7, Oil concentration= 15 ppm, PMS amount=30 mg/L, ZSM-5/TiO₂ nanocomposite amount= 15.00 K X, and in the presence of a UV lamp with a power of 15 W)

Effect of initial pH

The effect of solution pH on Oil removal using ZSM-5/TiO₂ nanocomposite is shown in Figure 5. In the experimental condition of Oil concentration of 15 ppm, PMS dose of 30 mg/L, and ZSM-5/TiO₂ nanocomposite dose of 30 mg/L, and in the presence of a UV lamp with a power of 15 W, the highest removal percentage was obtained 51.49% in the reaction time of 120 minutes for

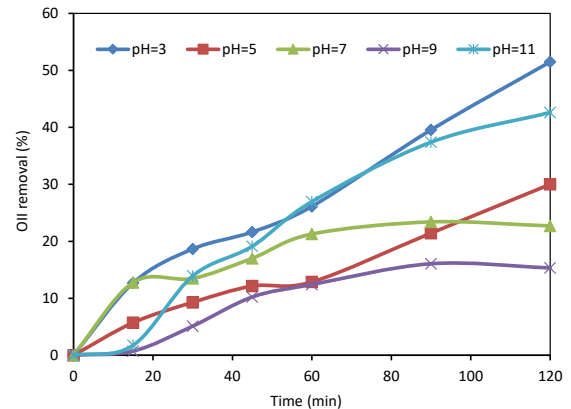


Figure 5. Effect of solution pH on Oil removal using ZSM-5/TiO₂ nanocomposite (the experimental conditions of Oil concentration= 15 ppm, PMS dose=30 mg/L, and nanocomposite dose=30 mg/L, in the presence of a UV lamp with a power of 15 W)

pH=3. As shown in Figure 5, the highest dye removal percentage is in an acidic environment (pH=3) and the lowest removal percentage is at pH=9.

Effect of initial Oil concentration

The effect of initial dye concentration on the removal of Oil using ZSM-5/TiO₂ nanocomposite is shown in Figure 6. The dye pollutant was investigated at the initial

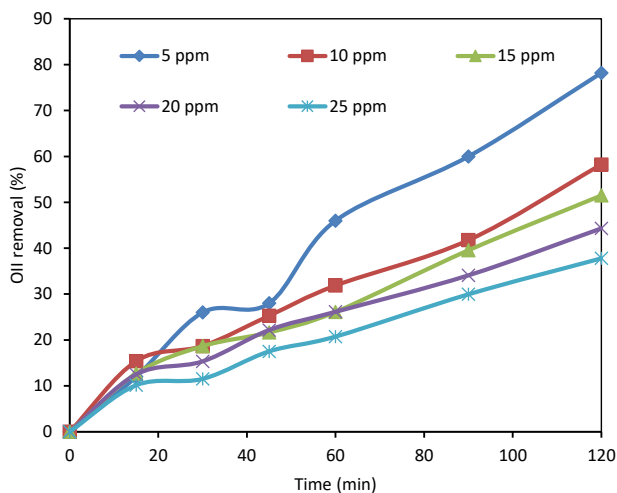


Figure 6. Effect of initial dye concentration on the removal of OII using ZSM-5/TiO₂ nanocomposite (the experimental condition of pH=3, PMS dose=30 mg/L, and TiO₂/ZSM-5 nanocomposite dose=30 mg/L, in the presence of a UV lamp with a power of 15 W)

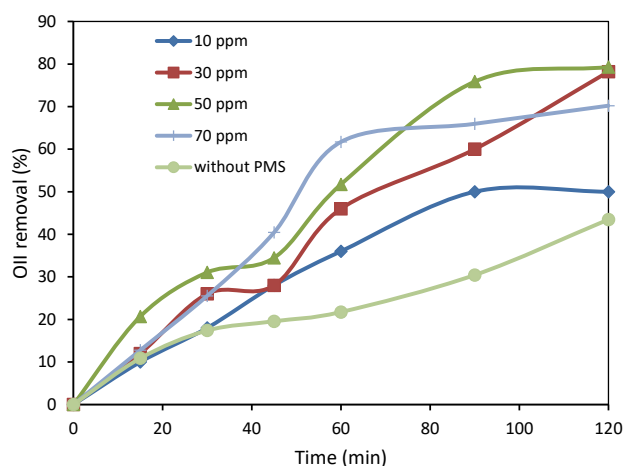


Figure 7. Effect of the PMS concentration on OII removal using ZSM-5/TiO₂ nanocomposite (the experimental condition of pH=3, pollutant concentration=5 ppm, and catalyst dose=30 mg/L, in the presence of a UV lamp with a power of 15 W)

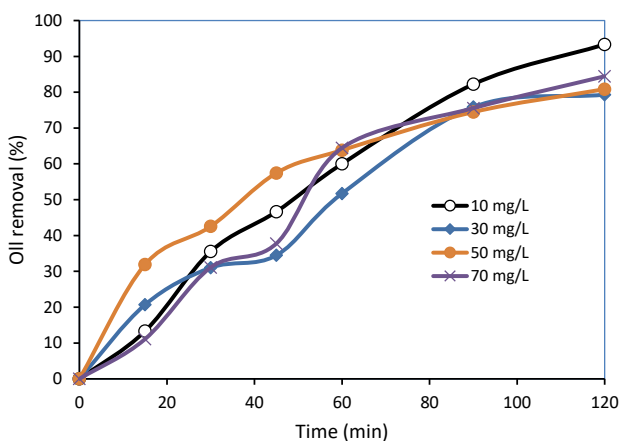


Figure 8. Effect of the TiO₂/ZSM-5 nanocomposite dosage on OII removal (the experimental condition of pH=3, pollutant concentration=5 ppm, and PMS dose=50 mg/L, in the presence of a UV lamp with a power of 15 W)

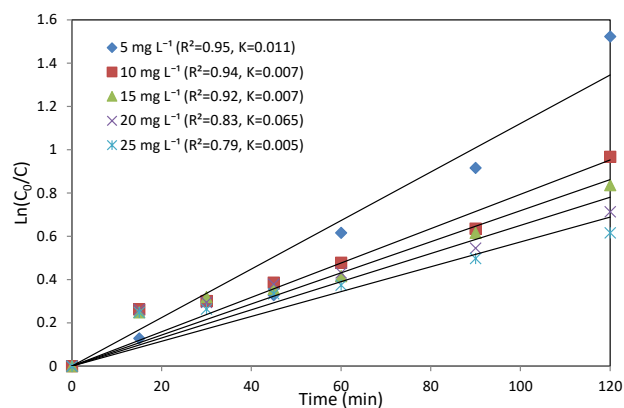


Figure 9. Kinetics of OII removal using ZSM-5/TiO₂ nanocomposite (the experimental condition of pH=3, pollutant concentration=5 ppm, nanocomposite dose=10 mg/L, and PMS dose=50 mg/L in the presence of a UV lamp with a power of 15 W)

concentrations of 5, 10, 15, 20, and 25 ppm, the best removal percentage is related to the dye with the lowest concentration (5 mg/L). In this test, the highest removal percentage was obtained to be 78.2% in the reaction time of 120 minutes for the OII initial concentration of 5 ppm and under conditions of pH=3, PMS dose=30 mg/L, and TiO₂/ZSM-5 nanocomposite dose=30 mg/L, in the presence of a UV lamp with a power of 15 W.

Effect of PMS concentration

Figure 7 shows the effect of the PMS concentration on OII removal using ZSM-5/TiO₂ nanocomposite. In this experiment, the highest removal percentage was obtained 79.31% in the reaction time of 120 minutes, for the PMS concentration of 50 mg/L and under the conditions of pH 3, pollutant concentration of 5 ppm, TiO₂/ZSM-5 nanocomposite dose of 30 mg/L, PMS dose of 10, 30, 50,

and 70 mg/L, and in the presence of a UV lamp with a power of 15 W (Figure 7).

Effect of TiO₂/ZSM-5 nanocomposite dosage

Figure 8 shows the nanocomposite concentration used for dye photocatalytic degradation. In this experiment, the highest removal percentage was 89.36% for the catalyst dose of 10 mg and under conditions of pH 3, pollutant concentration of 5 ppm, and TiO₂/ZSM-5 (200) nanocomposite dose of 10, 30, 50, and 70 mg/L, PMS dose of 50 mg/L, the reaction time of 120 minutes, and in the presence of a UV lamp with a power of 15 W.

Reaction kinetics

The photocatalytic degradation kinetics of OII dye with ZSM-5/TiO₂ zeolite was investigated and shown in Figure 9. The photocatalytic oxidation kinetics of many

Table 1. Comparative evaluation of photocatalytic removal of previous studies with the present study

Decomposition efficiency (%)	Decomposition time (min)	Catalyst type	light Source	Ref.
99.995	120	TiO ₂ /PMS	Xe-lamp (1000 W)	(27)
96.1	240	GO/Ag ₂ CrO ₄	Halogen-Tungsten lamp	(28)
95.4	180	Co-CeO ₂ NPs	200 W halogen	(29)
99.9	140	Cu/RGO	halogen lamp (400 W)	(30)
97.44	120	TiO ₂ /zeolite	UVA (15 W)	Present study

organic compounds is analyzed using the Langmuir–Hinshelwood (L–H) equation.

Comparative study

Table 1 shows the comparative evaluation of the percentage of OII removal with different photocatalysts in other studies with the present study.

Discussion

Characterization of the catalyst

Figures 1a and b show the XRD patterns of ZSM-5 zeolite and ZSM-5/TiO₂ nanocomposite, respectively. The peaks occurring at 2θ angles between 5-30 and 146 cm⁻¹ peak are related to the ZSM-5 zeolite structure in Figure 1a. The observed peaks at 2θ angles equal to 25/27, 38/05, 48/05, 55/04, and 54/09 in Figure 1b indicate the presence of TiO₂ on zeolite. The peaks between 5-10 and 64 degrees indicate the anatase phase and the peak at 31 degrees indicates the formation of the rutile TiO₂ phase (21).

Figures 2a and 2b show the spectra related to the FTIR analysis of ZSM-5 zeolite and TiO₂/ZSM-5 nanocomposite, respectively. The spectrum has an adsorption peak around 452, and 548, which is related to the Ti-O-Ti stretching bond in the TiO₂ structure. The adsorption peak observed in the wave number of 1637 indicates the Ti-O-H stretching bond between TiO₂ and zeolite. As can be observed, TiO₂ is placed in the structure of zeolite and the bond between them occurs (21).

BET is a powerful method to determine the porosity of porous materials, the average radius of the pores, and their specific surface area. This method is based on the adsorption of N₂ gas inside the holes. This method is based on the multi-layer adsorption of gas and measuring the volume of adsorbed and expelled gas using surface adsorption and expulsion charts (20). Table S1 shows the characteristics obtained from ZSM-5 Zeolite (316/20 m²/g) and TiO₂/ZSM-5 (200) (384/54 m²/g) nanocomposite through BET analysis. Table S1 indicates an increase in the surface of the holes and the total volume of the holes in the nanocomposite. The specific surface area and overall volume improved by adding TiO₂ to zeolite. The higher specific surface area indicates the more suitable adsorption sites in the substance, therefore, the adsorption and removal process also increased. So, TiO₂ can adsorb more photons, and then, more radicals are produced, and finally, dye removal happens better. Figure S1a and S1b show the diagram of nitrogen adsorption and desorption related to ZSM-5 zeolite and TiO₂/ZSM-5 nanocomposite,

respectively. According to the diagram, ZSM-5 zeolite and TiO₂/ZSM-5 nanocomposite have an isotherm of type IV. This kind of isotherm shows porous materials with narrow pores that have a distribution of meso-holes. In this type of porous material, the diameter of the holes is in the range of 2-50 nm (12).

Figures 3a, 3b, 3c, and 3d show images related to the SEM analysis of ZSM-5 samples (a and b) and TiO₂/ZSM-5 (200) nanocomposite. In Figure 3a and 3b, a sample of zeolite can be seen, which has a coffin-shaped structure. According to Figures 3c and 3d, the surface of the zeolite is porous and the nanoparticle distribution is completely uniform. It can also be observed that the existing unevenness increased the specific surface area of the material, which leads to an increase in the adsorption capacity and improved activity of the photocatalytic sites.

Figure 3d shows the presence of TiO₂ in the structure of zeolite ZSM-5. As shown in this figure, the morphology of zeolite did not change, only TiO₂ particles were placed on the surface of the zeolite and it led to a uniform distribution of the sample. The size of TiO₂ nanoparticles on zeolite was found to be 42 nm, which can be seen in Figure 3d.

EDS analysis was done to check the presence of elements in the sample. Figure S2 and Figure S3 show the elemental diagram of ZSM-5 zeolite and TiO₂/ZSM-5 nanocomposite, respectively. Tables S2 and S3 show the information about the mass percentage of zeolite and TiO₂/ZSM-5 nanocomposite, respectively. As shown in Figure S2, zeolite has elements including O, Na, Al, and Si. The elements O with 57.73% mass and Si with 38.52% mass are the main elements of zeolite, which are present in a few percentages of Na (1.82% mass) and Al (1.93% mass).

According to Figure S3, TiO₂/ZSM-5 nanocomposite, in addition to O, Na, Al, and Si, O element with a mass percentage of 62.15% and Si with a mass percentage of 23.67% are the main elements of zeolite, a significant percentage of Ti element (11.60%) was added to the main elements, which indicates the combination of TiO₂ with zeolite bonds. There are a few percentages of Na (1.37%) and Al (1.21%) in the composite structure.

Removal of OII

Effect of TiO₂ amount coated on zeolite

In Figure 4, it can be observed that with an increase in the ratio of TiO₂ coated on zeolite, the removal percentage increased, but after reaching a certain value (200 mg of

TiO₂ per 1 g of zeolite), this amount decreased. In this experiment, the highest removal percentage (22.69%) was obtained in 120 minutes. It was done under conditions of pH=7, OII concentration = 15 ppm, PMS amount = 30 mg/L, ZSM-5/TiO₂ nanocomposite amount = 30 mg/L, and in the presence of a UV lamp with a power of 15 W. As can be seen in Figure 4, with increasing TiO₂ loading on zeolite from 50 to 200 mg, the removal trend is upward and reached a high percentage. However, after passing the amount of 200 mg, the removal percentage decreases drastically. The reason for this is that increasing the load ratio on ZSM-5 reduces the porous space of zeolite and reduces the specific surface area of the catalyst. Furthermore, increasing the ratio of TiO₂ loading on ZSM-5 zeolite causes more activity of the TiO₂ and increases the hole electron, and ultimately, produces more OH radicals. Therefore, the value of 200 mg of TiO₂ per 1 gram of zeolite (TiO₂/ZSM-5 (200)) was chosen to continue the experiments.

Effect of initial pH

pH is one of the important factors affecting the amount and kind of surface charge. The isoelectric point refers to the pH at which the surface charge of the adsorbent becomes zero. At pHs higher than the mentioned point, the surface of the adsorbent becomes negatively charged, therefore, ions with the opposite charge (positive ions) are easily adsorbed, and also, at lower pHs, the surface charges become positive, and ion-negatively charged particles are adsorbed faster (31,32).

In this experiment, the highest removal percentage (51.49%) was obtained during 120 minutes reaction in pH=3, pollutant concentration of 15 ppm, PMS dose of 30 mg/L, ZSM-5/TiO₂ nanocomposite dose of 30 mg/L, and in the presence of a UV lamp with a power of 15 W. According to Figure 5, the highest dye removal percentage is in an acidic environment (pH=3) and the lowest one is related to pH 9. In an acidic environment, due to the release of H⁺, a positive surface charge was formed on the TiO₂/ZSM-5 nanocomposite (33). Furthermore, the acidic range increases the adsorption on the active sites due to the electrostatic attraction between the adsorbent and the adsorbed. The solution pH changes the electric charge of the interface of the solid electrolyte, as a result, it affects the processes of adsorption-desorption and separation of electron-hole pairs produced on the surface of semiconductor particles and the photocatalytic process. TiO₂ has amphoteric properties, thus, it can create a positive or negative charge on the surface. Therefore, pH change can affect the adsorption of dye molecules on TiO₂ surfaces. In alkaline pH, the electrostatic interaction between TiO₂ and OII cation leads to strong adsorption and high degradation rates (34). The photocatalyst at pH 11 acts similar to that at acidic pH (pH=3) and the removal percentage is high compared to that at neutral pH.

Effect of initial OII concentration

As shown in Figure 6, the dye pollutant was investigated at the initial concentrations of 5, 10, 15, 20, and 25 ppm, and the best removal percentage is related to the dye with the lowest concentration. In this test, the highest removal percentage was obtained 78.2% in the reaction time 120 minutes for the OII initial concentration of 5 ppm and under conditions of pH 3, PMS dose of 30 mg/L, and TiO₂/ZSM-5 nanocomposite dose of 30 mg/L, and it was done in the presence of UV lamp with 15 W power; it can be seen that with the increase of the initial concentration of OII dye, the removal efficiency decreased. This decrease in removal could be due to the lack of access of the pollutant at higher concentrations to the active sites of the adsorbent. Also, with the increase in pollutant concentration, the penetration of light into the solution and the active surface of the catalyst is disturbed, and it reduces the removal efficiency. It should also be noted that the oxidizing agent OH depends on the catalyst and light intensity, and with the increase in the concentration of the pollutant, the ratio of OH to the pollutant increases and the photocatalytic activity and removal efficiency decreases (35,36).

Effect of PMS concentration

PMS is known as an oxidizing agent and precursor for sulfate radicals. The addition of PMS can react with free electrons on TiO₂ surface to generate both SO₄^{-•} and •OH radicals and increase photocatalytic degradation (34). In this experiment, the highest removal percentage in 120 minutes of reaction time was obtained 79.31% for the PMS dose of 50 mg/L and under the conditions of pH 3, pollutant concentration of 5 ppm, and TiO₂/ZSM-5 nanocomposite dose of 30 mg/L, and PMS dose of 10, 30, 50, and 70 mg/L and in the presence of a UV lamp with a power of 15 W (Figure 7).

The addition of this substance increases the percentage of pollutant removal and after reaching an optimal value, adding more of this substance acts against the desired direction and reduces the percentage of pollutant removal. The addition of PMS helps to speed up the catalytic oxidation, however, an excessive dose of this substance may reduce the catalytic activity due to the scavenging of already-produced radicals. SO₄⁻² produced ions make the system corrosive and are not satisfactory (22,37).

Effect of TiO₂/ZSM-5 nanocomposite dosage

Figure 8 shows the amount of nanocomposite used for dye photocatalytic degradation. In this experiment, the highest removal percentage was obtained 89.36% in the reaction time of 120 minutes for the catalyst dose of 10 mg and under conditions of pH 3, pollutant concentration of 5 ppm, TiO₂/ZSM-5 (200) nanocomposite dose of 10, 30, 50, and 70 mg/L, and PMS dose of 50 mg/L, in the presence of a UV lamp with a power of 15 W.

It can be observed that adding more amounts of

nanocomposite decreases the removal percentage and the lowest concentration of catalyst has the best efficiency. Although the addition of high amounts of the catalyst increases the contact surface between the catalyst and the pollutant and surface adsorption, but with the increase in the concentration of the nano-catalyst, the water environment becomes cloudy and prevents the light from reaching the pollutant, and the photocatalytic degradation is prevented, and the process moves towards equilibrium. It is formed due to surface adsorption (38,39).

Reaction kinetics

In this study, the photocatalytic degradation kinetics of OII dye with ZSM-5/TiO₂ zeolite was investigated. The photocatalytic oxidation kinetics of many organic compounds is analyzed using the Langmuir–Hinshelwood (L–H) equation. The modified form of the equation is as follows (27):

$$r = \frac{dC}{dt} = \frac{kKC}{1+KC} \quad (1)$$

In this equation, r is the dye degradation rate, t is the degradation reaction time in minutes, C is the pollutant concentration, and k is the reaction rate constant. K is the absorption coefficient of dye on the photocatalyst particles. For low concentrations of reactants ($K \ll 1$), this value is removed from the above-mentioned equation and the equation after integration becomes as follows.

$$\ln \frac{C_0}{C} = kKt = K_{app}t \quad (2)$$

Here, C_0 is the initial dye concentration and K_{app} is the apparent rate constant. It was observed that the kinetics of photocatalytic degradation is pseudo-first-order (Figure 9).

Comparative study

In recent years, several studies have been conducted on the photocatalytic degradation of OII. Table 1 compares the percentage of OII removal with different photocatalysts in other research with the present study. As shown in this table, in the presence of UV light, the photocatalytic degradation percentage of dye by using the TiO₂/ZSM-5 (200) nanocomposite prepared in this study is an acceptable value and has a good position compared to other catalysts.

Conclusion

The photocatalytic degradation of OII was investigated using ZSM-5/TiO₂ nanocomposite for activation of PMS. The BET, XRD, SEM, EDS, and FTIR characterization were analyzed. According to the results, by adding TiO₂ nanoparticles to ZSM-5 zeolite, the specific surface and total volume increase, and the surface is improved. The highest rate of photocatalytic degradation was 97.44%

for optimal operating conditions, and the photocatalytic degradation of OII followed the pseudo-first-order kinetic according to Langmuir–Hinshelwood model. The role of ZSM-5/TiO₂ nanocomposite as a catalyst is important and it increases the speed of PMS activation, and as a result, it is effective in increasing the efficiency of the process.

Supplementary files

Supplementary file contains Figures S1-S3 and Table S1-S3.

Acknowledgments

The authors would like to thank Ilam University and Ilam University of Medical Sciences for their supports.

Authors' contributions

Conceptualization: Seyyed Abbas Mirzaee, Mohsen Mansouri, Zahra Noorimotlagh.

Data curation: Parisa Nasrollahi, Zeinab Gholami.

Formal Analysis: Parisa Nasrollahi, Zeinab Gholami.

Funding acquisition: Seyyed Abbas Mirzaee, Mohsen Mansouri, Zahra Noorimotlagh.

Investigation: Parisa Nasrollahi, Zeinab Gholami.

Methodology: Parisa Nasrollahi, Seyyed Abbas Mirzaee, Mohsen Mansouri.

Project administration: Mohsen Mansouri, Zahra Noorimotlagh.

Resources: Zahra Noorimotlagh.

Software: Zahra Noorimotlagh.

Supervision: Seyyed Abbas Mirzaee, Mohsen Mansouri, Zahra Noorimotlagh.

Validation: Seyyed Abbas Mirzaee, Mohsen Mansouri, Zahra Noorimotlagh.

Visualization: Zahra Noorimotlagh.

Writing–original draft: Parisa Nasrollahi, Zeinab Gholami, Mohsen Mansouri, Zahra Noorimotlagh.

Writing–review & editing: Parisa Nasrollahi, Seyyed Abbas Mirzaee, Zeinab Gholami, Mohsen Mansouri, Zahra Noorimotlagh.

Competing interests

The authors of this research declare no conflict of interests.

Ethical issues

This study is a part of the thesis of Parisa Nasrollahi at Ilam University (IranDoc Code: 1641461).

References

- Nasiri A, Tamaddon F, Mosslemin MH, Amiri Gharaghani M, Asadipour A. Magnetic nano-biocomposite CuFe₂O₄@methylcellulose (MC) prepared as a new nano-photocatalyst for degradation of ciprofloxacin from aqueous solution. *Environ Health Eng Manag.* 2019;6(1):41-51. doi: 10.15171/ehem.2019.05.
- Malakootian M, Nasiri A, Heidari MR. Removal of phenol from steel plant wastewater in three dimensional

- electrochemical (TDE) process using CoFe₂O₄@AC/H₂O₂. *Z Phys Chem (N F)*. 2020;234(10):1661-79. doi: [10.1515/zpch-2019-1499](https://doi.org/10.1515/zpch-2019-1499).
3. Deniz F, Mazmanlı MA. Advanced oxidation of high concentrations of formaldehyde in aqueous solution under fluorescent and UV light. *Environ Health Eng Manag*. 2021;8(4):267-76. doi: [10.34172/ehem.2021.30](https://doi.org/10.34172/ehem.2021.30).
 4. Chiu YH, Chang TF, Chen CY, Sone M, Hsu YJ. Mechanistic insights into photodegradation of organic dyes using heterostructure photocatalysts. *Catalysts*. 2019;9(5):430. doi: [10.3390/catal9050430](https://doi.org/10.3390/catal9050430).
 5. Noorimotlagh Z, Darvishi Cheshmeh Soltani R, Shams Khorramabadi G, Godini H, Almasian M. Performance of wastewater sludge modified with zinc oxide nanoparticles in the removal of methylene blue from aqueous solutions. *Desalin Water Treat*. 2016;57(4):1684-92. doi: [10.1080/19443994.2014.977954](https://doi.org/10.1080/19443994.2014.977954).
 6. Eslami H, Ehrampoush MH, Esmaeili A, Ebrahimi AA, Salmani MH, Ghaneian MT, et al. Efficient photocatalytic oxidation of arsenite from contaminated water by Fe₂O₃-Mn₂O₃ nanocomposite under UVA radiation and process optimization with experimental design. *Chemosphere*. 2018;207:303-12. doi: [10.1016/j.chemosphere.2018.05.106](https://doi.org/10.1016/j.chemosphere.2018.05.106).
 7. Malakootian M, Smith A Jr, Amiri Gharaghani M, Mahdizadeh H, Nasiri A, Yazdanpanah G. Decoloration of textile acid red 18 dye by hybrid UV/COP advanced oxidation process using ZnO as a catalyst immobilized on a stone surface. *Desalin Water Treat*. 2020;182:385-94. doi: [10.5004/dwt.2020.25216](https://doi.org/10.5004/dwt.2020.25216).
 8. Naseem K, Farooqi ZH, Begum R, Wu W, Irfan A, Al-Sehemi AG. Silver nanoparticles engineered polystyrene-poly(N-isopropylmethacrylamide-acrylic acid) core shell hybrid polymer microgels for catalytic reduction of Congo red. *Macromol Chem Phys*. 2018;219(18):1800211. doi: [10.1002/macp.201800211](https://doi.org/10.1002/macp.201800211).
 9. Nikoonahad A, Djahed B, Norzaee S, Eslami H, Derakhshan Z, Miri M, et al. An overview report on the application of heteropoly acids on supporting materials in the photocatalytic degradation of organic pollutants from aqueous solutions. *PeerJ*. 2018;6:e5501. doi: [10.7717/peerj.5501](https://doi.org/10.7717/peerj.5501).
 10. Eslami H, Shariatifar A, Rafiee E, Shiranian M, Salehi F, Hosseini SS, et al. Decolorization and biodegradation of reactive red 198 Azo dye by a new *Enterococcus faecalis*-*Klebsiella variicola* bacterial consortium isolated from textile wastewater sludge. *World J Microbiol Biotechnol*. 2019;35(3):38. doi: [10.1007/s11274-019-2608-y](https://doi.org/10.1007/s11274-019-2608-y).
 11. Hama Aziz KH, Miessner H, Mueller S, Mahyar A, Kalass D, Moeller D, et al. Comparative study on 2,4-dichlorophenoxyacetic acid and 2,4-dichlorophenol removal from aqueous solutions via ozonation, photocatalysis and non-thermal plasma using a planar falling film reactor. *J Hazard Mater*. 2018;343:107-15. doi: [10.1016/j.jhazmat.2017.09.025](https://doi.org/10.1016/j.jhazmat.2017.09.025).
 12. Anandan S, Yoon M. Photocatalytic activities of the nano-sized TiO₂-supported Y-zeolites. *J Photochem Photobiol C Photochem Rev*. 2003;4(1):5-18. doi: [10.1016/s1389-5567\(03\)00002-9](https://doi.org/10.1016/s1389-5567(03)00002-9).
 13. Noorimotlagh Z, Ravanbakhsh M, Valizadeh MR, Bayati B, Kyzas GZ, Ahmadi M, et al. Optimization and genetic programming modeling of humic acid adsorption onto prepared activated carbon and modified by multi-wall carbon nanotubes. *Polyhedron*. 2020;179:114354. doi: [10.1016/j.poly.2020.114354](https://doi.org/10.1016/j.poly.2020.114354).
 14. Yu Y, Zhao C, Liu X, Sui M, Meng Y. Selective flocculation of pollutants in wastewater using pH responsive HM-alginate/chitosan complexes. *J Environ Chem Eng*. 2017;5(6):5406-10. doi: [10.1016/j.jece.2017.10.025](https://doi.org/10.1016/j.jece.2017.10.025).
 15. Noorimotlagh Z, Dehviri M, Mirzaee SA, Jaafarzadeh N, Silva-Martinez S, Amarloe A. Efficient sonocatalytic degradation of orange II dye and real textile wastewater using peroxymonosulfate activated with a novel heterogeneous TiO₂-FeZn bimetallic nanocatalyst. *J Iran Chem Soc*. 2023;20(7):1589-603. doi: [10.1007/s13738-023-02780-3](https://doi.org/10.1007/s13738-023-02780-3).
 16. Noorimotlagh Z, Kazeminezhad I, Jaafarzadeh N, Ahmadi M, Ramezani Z. Improved performance of immobilized TiO₂ under visible light for the commercial surfactant degradation: role of carbon doped TiO₂ and anatase/rutile ratio. *Catal Today*. 2020;348:277-89. doi: [10.1016/j.cattod.2019.08.051](https://doi.org/10.1016/j.cattod.2019.08.051).
 17. Mirzaee SA, Jaafarzadeh N, Gomes HT, Jorfi S, Ahmadi M. Magnetic titanium/carbon nanotube nanocomposite catalyst for oxidative degradation of bisphenol A from high saline polycarbonate plant effluent using catalytic wet peroxide oxidation. *Chem Eng J*. 2019;370:372-86. doi: [10.1016/j.cej.2019.03.202](https://doi.org/10.1016/j.cej.2019.03.202).
 18. Noorimotlagh Z, Kazeminezhad I, Jaafarzadeh N, Ahmadi M, Ramezani Z, Silva-Martinez S. The visible-light photodegradation of nonylphenol in the presence of carbon-doped TiO₂ with rutile/anatase ratio coated on GAC: effect of parameters and degradation mechanism. *J Hazard Mater*. 2018;350:108-20. doi: [10.1016/j.jhazmat.2018.02.022](https://doi.org/10.1016/j.jhazmat.2018.02.022).
 19. Ichiura H, Kitaoka T, Tanaka H. Preparation of composite TiO₂-zeolite sheets using a papermaking technique and their application to environmental improvement part I removal of acetaldehyde with and without UV irradiation. *J Mater Sci*. 2002;37(14):2937-41. doi: [10.1023/a:1016060729376](https://doi.org/10.1023/a:1016060729376).
 20. Guesh K, Mayoral Á, Márquez-Álvarez C, Chebude Y, Díaz I. Enhanced photocatalytic activity of TiO₂ supported on zeolites tested in real wastewaters from the textile industry of Ethiopia. *Microporous Mesoporous Mater*. 2016;225:88-97. doi: [10.1016/j.micromeso.2015.12.001](https://doi.org/10.1016/j.micromeso.2015.12.001).
 21. Mian MM, Liu G. Activation of peroxymonosulfate by chemically modified sludge biochar for the removal of organic pollutants: understanding the role of active sites and mechanism. *Chem Eng J*. 2020;392:123681. doi: [10.1016/j.cej.2019.123681](https://doi.org/10.1016/j.cej.2019.123681).
 22. Duan L, Sun B, Wei M, Luo S, Pan F, Xu A, et al. Catalytic degradation of acid orange 7 by manganese oxide octahedral molecular sieves with peroxymonosulfate under visible light irradiation. *J Hazard Mater*. 2015;285:356-65. doi: [10.1016/j.jhazmat.2014.12.015](https://doi.org/10.1016/j.jhazmat.2014.12.015).
 23. Liu F, Yi P, Wang X, Gao H, Zhang H. Degradation of acid orange 7 by an ultrasound/ZnO-GAC/persulfate process. *Sep Purif Technol*. 2018;194:181-7. doi: [10.1016/j.seppur.2017.10.072](https://doi.org/10.1016/j.seppur.2017.10.072).
 24. Nasiri A, Malakootian M, Heidari MR, Asadzadeh SN. CoFe₂O₄@methylcellulose as a new magnetic nano biocomposite for sonocatalytic degradation of reactive blue 19. *J Polym Environ*. 2021;29(8):2660-75. doi: [10.1007/s10924-021-02074-w](https://doi.org/10.1007/s10924-021-02074-w).
 25. Hao X, Wang G, Chen S, Yu H, Quan X. Enhanced activation of peroxymonosulfate by CNT-TiO₂ under UV-light assistance for efficient degradation of organic pollutants. *Front Environ Sci Eng*. 2019;13(5):77. doi: [10.1007/s11783-](https://doi.org/10.1007/s11783-)

- 019-1161-0.
26. Chen X, Wang W, Xiao H, Hong C, Zhu F, Yao Y, et al. Accelerated TiO₂ photocatalytic degradation of acid orange 7 under visible light mediated by peroxymonosulfate. *Chem Eng J*. 2012;193-194:290-5. doi: [10.1016/j.cej.2012.04.033](https://doi.org/10.1016/j.cej.2012.04.033).
 27. Nouri H, Habibi-Yangjeh A, Azadi M. Preparation of Ag/ZnMgO nanocomposites as novel highly efficient photocatalysts by one-pot method under microwave irradiation. *J Photochem Photobiol A Chem*. 2014;281:59-67. doi: [10.1016/j.jphotochem.2014.03.006](https://doi.org/10.1016/j.jphotochem.2014.03.006).
 28. Hamidian K, Najafidoust A, Miri A, Sarani M. Photocatalytic performance on degradation of acid orange 7 dye using biosynthesized un-doped and Co doped CeO₂ nanoparticles. *Mater Res Bull*. 2021;138:111206. doi: [10.1016/j.materresbull.2021.111206](https://doi.org/10.1016/j.materresbull.2021.111206).
 29. Saber Khatibi E, Haghghi M, Mahboob S. Efficient surface design of reduced graphene oxide, carbon nanotube and carbon active with copper nanocrystals for enhanced simulated-solar-light photocatalytic degradation of acid orange in water. *Appl Surf Sci*. 2019;465:937-49. doi: [10.1016/j.apsusc.2018.09.225](https://doi.org/10.1016/j.apsusc.2018.09.225).
 30. Han JS, Hur N, Choi B, Min SH. Removal of phosphorus using chemically modified lignocellulosic materials. In: *Proceedings of the 6th Inter Regional Conference on Environment-Water, "Land and Water Use Planning and Management"*. Albacete, Spain: CREA; 2003.
 31. Jaafarzadeh N, Baboli Z, Noorimotlagh Z, Silva-Martínez S, Ahmadi M, Alavi S, et al. Efficient adsorption of bisphenol A from aqueous solutions using low-cost activated carbons produced from natural and synthetic carbonaceous materials. *Desalin Water Treat*. 2019;154:177-87. doi: [10.5004/dwt.2019.23897](https://doi.org/10.5004/dwt.2019.23897).
 32. Piedra López JG, González Pichardo OH, Pinedo Escobar JA, de Haro del Río DA, Inchaurregui Méndez H, González Rodríguez LM. Photocatalytic degradation of metoprolol in aqueous medium using a TiO₂/natural zeolite composite. *Fuel*. 2021;284:119030. doi: [10.1016/j.fuel.2020.119030](https://doi.org/10.1016/j.fuel.2020.119030).
 33. Jiang Y, Wang H, Chen Y, He J, Chen L, Liu Y, et al. Clinical data on hospital environmental hygiene monitoring and medical staff protection during the coronavirus disease 2019 outbreak. medRxiv [Preprint]. March 2, 2020. Available from: <https://www.medrxiv.org/content/10.1101/2020.02.25.20028043v2>.
 34. Daneshvar N, Rasoulifard MH, Khataee AR, Hosseinzadeh F. Removal of C.I. Acid orange 7 from aqueous solution by UV irradiation in the presence of ZnO nanopowder. *J Hazard Mater*. 2007;143(1):95-101. doi: [10.1016/j.jhazmat.2006.08.072](https://doi.org/10.1016/j.jhazmat.2006.08.072).
 35. Noorimotlagh Z, Mirzaee SA, Silva-Martínez S, Alavi S, Ahmadi M, Jaafarzadeh N. Adsorption of textile dye in activated carbons prepared from DVD and CD wastes modified with multi-wall carbon nanotubes: equilibrium isotherms, kinetics and thermodynamic study. *Chem Eng Res Des*. 2019;141:290-301. doi: [10.1016/j.cherd.2018.11.007](https://doi.org/10.1016/j.cherd.2018.11.007).
 36. Daneshvar N, Salari D, Khataee AR. Photocatalytic degradation of azo dye acid red 14 in water on ZnO as an alternative catalyst to TiO₂. *J Photochem Photobiol A Chem*. 2004;162(2-3):317-22. doi: [10.1016/s1010-6030\(03\)00378-2](https://doi.org/10.1016/s1010-6030(03)00378-2).
 37. Zhang LS, Wong KH, Yip HY, Hu C, Yu JC, Chan CY, et al. Effective photocatalytic disinfection of *E. coli* K-12 using AgBr-Ag-Bi₂WO₆ nanojunction system irradiated by visible light: the role of diffusing hydroxyl radicals. *Environ Sci Technol*. 2010;44(4):1392-8. doi: [10.1021/es903087w](https://doi.org/10.1021/es903087w).
 38. Nakhaei Pour M, Rangkooy HA, Jahani F, Golbaghi A, Shojaee-Farah Abady H, Nematpour L. Removal of styrene by the synthesized ZnO nanoparticles coated on the activated carbon adsorbent in the presence of UV irradiation. *Environ Health Eng Manag*. 2019;6(4):225-32. doi: [10.15171/ehem.2019.25](https://doi.org/10.15171/ehem.2019.25).